Anion−Anion Assembly in Crystal of Sodium Nitroprusside

Yulia V. Nelyubina,[†] Konstantin A. Lyssenko,*[,†] Vitalii Yu. Kotov,[‡] and Mikhail Yu. Antipin[†]

A. N. Nesmeyanov Institute of Organoelement Compounds, Russian Academy of Sciences, 119991, Vavilov Str., 28, Moscow, Russia, and Department of Chemistry and Biology, Moscow City Pedagogical University, 105568, Chechulina str., 1, Moscow, Russia

Received: April 18, 2008; Revised Manuscript Received: June 19, 2008

The experimental charge density in the crystal of disodium pentacyanonitrosoferrate (sodium nitroprusside) dihydrate was analyzed in detail by means of Bader's atoms in molecules theory. It was shown that nitroprusside anion is involved in relatively strong self-interactions through the nitroso group. The obtained results agree well with the spectroscopic data, indicating the tendency of the corresponding moiety to the formation of anion−anion association both in solutions and in the crystalline phase.

Introduction

One of the most confusing aspects of binding in ionic crystals is the occurrence of shortened contacts between likely charged moieties. Such effect is usually attributed to the formation of cation−anion interactions, which force anions (cations) to be placed at the distance that is shorter than the sum of van der Waals radii of "touching" atoms.[1] Postulating the fact that the ions with the same sign of charge repel each other, the majority of investigators do not consider such arrangement as an indicator of chemical bonding. On the other hand, the aggregates linked via interactions of likely charged moieties exhibit not only similar geometrical but also similar spectroscopic properties (e.g., luminescence) as energetically stable ion pairs.[2] Thus, it is possible to detect the association of the likely charged ions in solids via analysis of the electronic absorption (EAS) spectra for the particular crystalline material. This approach has revealed the presence of cation−cation interactions in various actinide salts containing AnO_2^+ or AnO_2^{2+} groups hold together by An···O contacts.[3] In all cases such binding leads to a bathochromic shift in EAS spectra for the crystals relative to those for solutions. The value of the shift, in turn, depends on both the number of cation−cation interactions in the solid and the type of supramolecular patterns resulted from their formation. In addition, EAS was successfully applied to ionic systems containing complex anion, e.g., hexacyanoferrate or ethylendiamintetraacetatocobaltate,[4] and one being the reducing agent such as I^-, $S_2O_3^{2-}$, and the like. The presence of additional charge transfer band in the corresponding spectra was found to be indicative of anion−anion association in the crystalline phase[5] as well as in aqueous solutions.[4] Along with the routine X-ray diffraction and EAS studies, the existence of interactions between the likely charged moieties has been also supported by IR spectroscopy[3] and NMR data.[6]

Unfortunately, the key feature of the above methods is that they provide only qualitative description of such assembly. The usage of a more sophisticated approach based on a detailed examination of electron density distribution $\rho(\mathbf{r})$ in crystal[7−9] by means of Bader's atoms in molecules (AIM) theory[10] does not suffer from this drawback. It gives the opportunity to check whether or not the shortened contacts between anions (cations) correspond to bonding (attractive) interactions based on the presence of local minima in the $\rho(\mathbf{r})$ function, so-called bond critical points (3, −1) or BCPs.[10] In addition this method allows to characterize the thus-revealed interactions on the quantitative level.[11,12] In particular, using the AIM analysis of $\rho(\mathbf{r})$ function derived from the accurate X-ray diffraction (XRD) data anion−anion interactions were found,[13−18] and their energy was estimated, for instance, in the case of crystalline hydroxylammonium chloride,[19] danburite,[20] urea nitrate,[21] and sodium chlorate.[22] The main problem arising in the previous studies is that the information obtained in such a way has not been proved by any other physical chemical method.

Therefore, the topological analysis of $\rho(\mathbf{r})$ in crystal of the ionic compound, which was previously investigated by EAS, is known to exhibit anion−anion interactions. We have chosen disodium pentacyanonitrosoferrate (sodium nitroprusside) dihydrate (**1**) for our study due to the shortened O···O contacts (2.6423(5) Å) between neighboring anions in the solid state.[23] In addition, the available dynamic deformation electron density maps and the results of thermal motion analysis clearly show that **1** is fully ordered and thus is absolutely suitable for the detailed analysis of its chemical bonding peculiarities.[24] Moreover, the spectroscopic studies of different liquid systems $[FeNO(CN)_5]^{2-}$−X (X is anionic reducing agent) has indicated the anion−anion association occurring through the nitroso fragment.[25,26] To pool the EAS and XRD results concerning the binding of like-charged moieties in **1** we have performed the AIM analysis of the $\rho(\mathbf{r})$ based on high-resolution XRD data for the corresponding crystal.

Experimental Section

Crystals of **1** ($C_5H_4FeN_6Na_2O_3$, M = 297.97) are orthorhombic, space group *Pnnm*, at 100 K $a = 6.1408(3)$, $b = 11.8484(5)$, $c = 15.5454(7)$ Å, $V = 1131.06(9)$ Å^3, $Z = 4$ ($Z' = 1/2$), $d_{calc} = 1.750$ g cm^{-3}, μ(Mo Kα) = 14.14 cm^{-1}, $F(000) = 592$. Intensities of 133727 reflections were measured with a Bruker SMART APEX2 CCD diffractometer [λ(Mo Kα) = 0.71072Å, ω-scans, $2\theta < 115°$], and 8041 independent reflections [$R_{int} = 0.0498$] were used in further refinement. The structure was solved by direct method and refined using the full-matrix least-squares technique against F^2 in the anisotropic−isotropic approximation. Hydrogen atoms were located using the Fourier

* To whom correspondence should be addressed. E-mail: kostya@xrlab.ineos.ac.ru.
† Russian Academy of Sciences.
‡ Moscow City Pedagogical University.

10.1021/jp803394f CCC: $40.75
Published on Web 08/27/2008

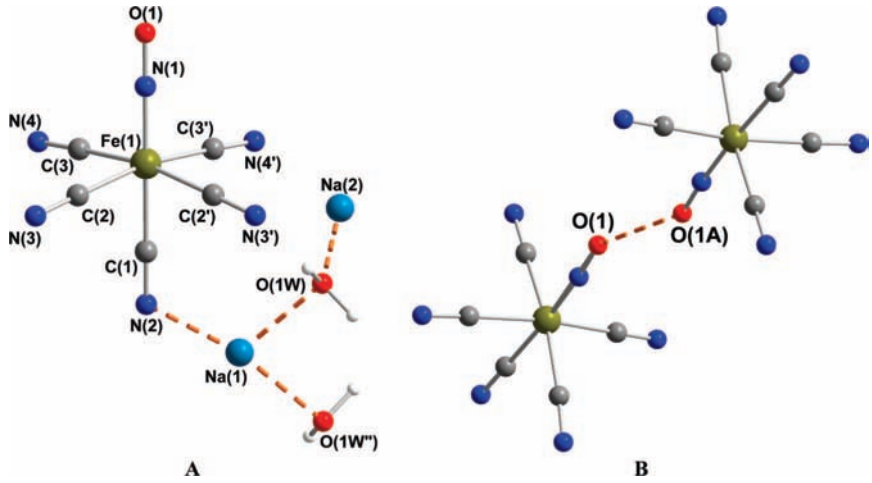

Figure 1. The general view of **1** (**A**) and the fragment of its crystal packing (**B**), representing the formation of the O···O contact. The atoms with an asterisk are obtained from the basic ones by the symmetry operation $-x, -y, -z$; O(1W″) (**A**) and O(1A) (**B**) atoms by $-x + 1, -y + 1, -z$, and $-x - 1, -y + 2, -z + 1$.

synthesis of the electron density and refined in the isotropic approximation. For **1** the refinement converged to $wR2 = 0.0691$ and GOF = 1.010 for all independent reflections ($R1 = 0.0255$ was calculated against F for 5933 observed reflections with $I > 2\sigma(I)$). All calculations were performed using SHELXTL PLUS 5.0. CCDC 684170 contains the supplementary crystallographic data for **1**.[27]

The multipole refinement was carried out within the Hansen−Coppens formalism[28] using the XD program package[29] with the core and valence electron density derived from wave functions fitted to a relativistic Dirac−Fock solution.[30] Before the refinement the O−H bond distances were normalized to the values obtained from the neutron data.[23] The level of multipole expansion was hexadecapole for iron and octupole for other non-hydrogen atoms. The refinement was carried out against F and converged to $R = 0.0159$, $Rw = 0.0132$, and GOF = 0.944 for 5022 merged reflections with $I > 3\sigma(I)$). All bonded pairs of atoms satisfy the Hirshfeld rigid-bond criteria. The potential energy density $v(\mathbf{r})$ was evaluated through the Kirzhnits approximation[31] for the kinetic energy density function $g(\mathbf{r})$. Accordingly, the $g(\mathbf{r})$ function is described as $(3/10)(3\pi^2)^{2/3}[\rho(\mathbf{r})]^{5/3} + (1/72)|\nabla\rho(\mathbf{r})|^2/\rho(\mathbf{r}) + 1/6\nabla^2\rho(\mathbf{r})$, which in conjunction with the local virial theorem ($2g(\mathbf{r}) + v(\mathbf{r}) = {}^1/_4\nabla^2\rho(\mathbf{r})$) leads to the expression for v($\mathbf{r}$) and makes possible to estimate the electronic energy density $h_e(\mathbf{r})$. The total electron density function was positive everywhere and the maxima of residual electron density located in the vicinity of nuclei were not more that 0.21 eÅ^{-3}. Analysis of topology of the $\rho(\mathbf{r})$ function was carried out using the WinXPRO program package.[32]

DFT and ab intio calculations of the isolated anion **1** were performed with the Gaussian98 program package using different functionals (B3LYP, B3PW91) and at the MP2 level of theory. Full optimization of the anion at the C_1 point group was carried out with the 6-311G* basis set starting from the X-ray structural data. The extremely tight threshold limits of 2×10^{-6} and 6×10^{-6} au were applied for the maximum force and displacement, respectively. To account for the solvent effect, we also performed calculations at B3PW91 level using the polarizable continuum (SCRF/PCM) model,[33] with water ($\varepsilon = 78.39$) as a solvent. The topological analysis of the computed electron densities was performed using MORPHY 98 and AIM2000 program packages.[34]

Potentiometric investigation of ion association in solution was performed with the ion-meter EXPERT-001 (Econix-Expert, Ltd.) and sodium-selective electrodes ELIS-112 Na. Measurements were carried out in the measuring range of milivoltmeter at 302 K. The accuracy was 0.1 mV. As an activity reference standard for sodium ions the NaCl solutions were used. The concentration values were estimated from the corresponding activities using the reference data.

Results and Discussion

Geometrical Considerations. The XRD analysis reveals the distorted octahedral geometry of the iron center in **1** (Figure 1A). Although the main distortion is caused by the presence of NO group (Fe−N = 1.6644(5) Å), the Fe−C bond lengths are also different (1.9233(6)−1.9386(4) Å). The slight elongation of the Fe(1)−C(2) and C(2)−N(3) bonds (1.1610(6) Å) as compared to the rest of the independent C−N fragments (1.1582(8) and 1.1594(6) Å) cannot be explained by intramolecular effects. It follows from the crystal packing that the major difference between the cyano moieties is due to the number of cation−anion bonds. The C(2)N(3) group is bound to only one sodium atom (the Na···N distance is 2.4702(6) Å), while the others are coordinated by two cations, namely, two symmetry equivalent Na(1) atoms in the case of C(1)N(2) fragment (Na···N 2.4733(5) Å) and both Na(1) and Na(2) atoms for C(3)N(4) one (Na···N = 2.4704(5)−2.5083(7) Å). These contacts along with the Na−O interactions, which hold cations of **1** and water molecules together (the Na···O distance varies from 2.4721(6) to 2.5084(6) Å), lead to formation of a 3D framework. Moreover, the specific organization of ions in the crystal **1** results in shortened anion−anion contacts (Figure 1B).

On the basis of the geometrical criteria one can expect the neighboring anions to be linked by two types of interactions, namely O···O (2.6423(5) Å) and O···CN (3.1482(5) Å). According to the Cambridge Structural Database (CSD) the former one can be considered a common feature of nitroso compounds (137 ordered structures with O···O distance between 2.5 and 3.1 Å), whereas the latter interaction is rather rare. Only five structures contain both NO and CN fragments with O···C and O···N distances of 2.7−3.3 Å. One notes that NO groups involved in the formation of anion−anion contacts of O···O type tend to orient themselves in a specific manner so that 25% of the reported nitroso-containing compounds show the value of the N−O···O angle varying from 89.7 to 91.8°. In addition, the mean value of the N−O···O angle (144.9°) is

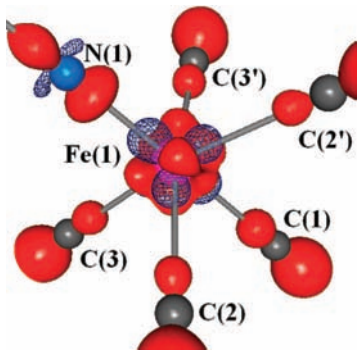

Figure 2. The 3D distribution of DED around the Fe(1) atom in **1**. Isosurface of DED equal to 0.3 eÅ^{-3} is shown by red; the negative isosurface (DED is −0.3 eÅ^{-3}) is shown by wireframe.

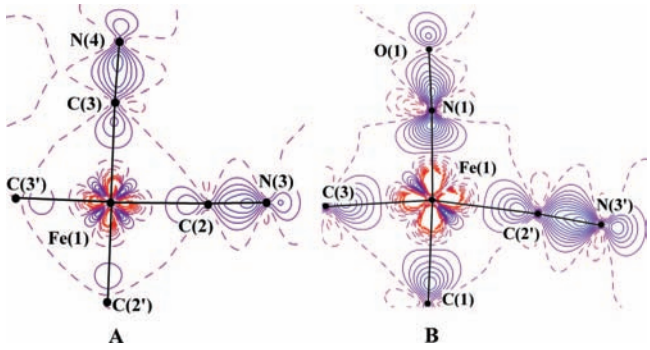

Figure 3. The DED distributions in the section of $Fe(CN)_4$ distorted square (**A**) and in the perpendicular plane (**B**) in the crystal of **1**. The contours are drawn with 0.1 eÅ^{-3} interval; the nonpositive contours are dashed. The atoms with prime are obtained from the basic ones by the symmetry operation $x, y, -z + 1$.

observed in a number of species, which exhibit the most shortened O···O contacts (with distances very close to sum of van der Waals radii of oxygen and equal to 2.54−2.72 Å). This is similar to that in the crystal of **1** (151.6(1)°). Although some authors admitted the unusual aggregation of nitroprusside anions in the solid,[35] this effect has not been analyzed. Nevertheless, such mutual disposition of likely charged moieties can be indicative of chemical binding between them. One can expect the anion−anion interactions formed by nitroso fragments in **1** to be rather strong. Indeed, similar O···O assembly (O···O = 2.32−3.36 Å) in the crystalline urea nitrate[21] and danburite[20] is characterized by relatively high bonding energy of 1.6−16.3 kcal/mol. On the other hand, the longer O···CN contacts (with account for the difference between oxygen and carbon atomic radii) seem to be very weak or even forced in nature. To analyze the nature of these bonds and their energetics, the topological analysis of experimental $\rho(\mathbf{r})$ function in this particular crystal has been performed.

Binding within the Anionic Moiety. The qualitative examination of the static deformation electron density (DED) distribution for the complex anion revealed that the latter is characterized by expected features, in particular by the significant anisotropy of DED around the iron atom (Figures 2 and 3). This is a common trend for crystalline complexes of 3d-metals and has been previously observed in dynamic DED maps for **1**.[24] Unfortunately, we cannot examine the 3d orbital population on the quantitative level because according to the previously reported data for analogous ruthenium complexes[36] the d_{z^2} orbital of the metal center that is π^* with respect to the ML fragment is directed toward the NO group. On the other hand, the local symmetry restrictions, i.e., site symmetry of the anion (mirror plane),[37] do not allow to direct the z axis along the Fe−NO bond and thus to calculate 3d orbital occupancies. Thus, we have limited our orbital population analysis to the qualitative description of DED distribution around the iron atom in **1**, which is independent of the local coordinate system.

The maxima of DED around Fe(1) form the distorted cube with the vertices directed toward the triangular faces of the iron coordination polyhedron. The area of its depletion, which can be considered antibonding d_{z^2} and d_{xy} orbitals, are located along the Fe−X bond lines. The main distortion of the cubic electron distribution is observed for the section of DED accumulation attributed to the most populated (according to the $\rho(\mathbf{r})$ values at CP (3, −3) of $\nabla^2\rho(\mathbf{r})$ function) d_{yz} and/or d_{xz} orbitals of the metal atom. Such polarization of the valence shell of Fe toward the O(1)C(2)C(2′) face and toward the opposite side of the octahedron is, apparently, due to the crystal packing effects.

One notes that the octahedral surrounding of Fe(1) is reflected not only in a similarity of geometrical parameters of the Fe−NO and Fe−CN fragments but also in a qualitative accord of the corresponding DED sections (Figure 3). Thus, in both cases the Fe−X (X = C or N) bonds correspond to "peak to hole" type of interactions, i.e., the regions of charge accumulation near the inner atoms of nitroso and cyano groups are extended toward the areas of its depletion at the iron site. For instance, one of the NO fragments in crystalline dinitrosyl iron complex with 1,2,4-triazole-3-thione as a ligand exhibits the same electron density distribution.[38] The presence of one DED maximum in **1** (Figure 3) is attributed to the electron lone pair in the vicinity of each terminal atom (oxygen or nitrogen). This feature is compatible with the triple character of both N−O and C−N bonds and single bond for Fe−N and Fe−C bonds. Such distribution is consistent with the ellipticity (ε) values in BCPs for these bonds (ε = 0.02−0.07). This shows no significant deviation of their symmetry from the cylindrical one.[10] For the intraionic Fe−C and Fe−N interactions the small ε values reflect a slight back-donation similar to the case of Fe−NO bonding (ε = 0.08 and 0.11) in the above dinitrosyl complex.[38] Despite similar ε values for Fe−N and Fe−C interactions, their other topological parameters remarkably vary. The values of $\rho(\mathbf{r})$ and $\nabla^2\rho(\mathbf{r})$ functions in BCPs are equal to 1.243 and 0.751−0.779 eÅ^{-3} for the Fe−N bonds, whereas in the case of Fe−C they equal 2.36 and 7.61−7.84 eÅ^{-5}, respectively. Nevertheless, both Fe−N and Fe−C bonds correspond to the intermediate type of interatomic interactions with the positive $\nabla^2\rho(\mathbf{r})$ and negative electron energy density ($h_e(\mathbf{r})$ is from −0.08963 to −0.04753 au). This type of bonding has been previously reported for the Fe−NO[38] and Ru−NO[39] interactions in the tetrahedral as well as octahedral complex ions with the $\rho(\mathbf{r})$, $\nabla^2\rho(\mathbf{r})$ and $h_e(\mathbf{r})$ values in BCPs varying only slightly. The component of the covalent character of the intraionic bonds in **1** linking the iron center with CN or NO ligands in the notation of Espinosa's classification of bonded interactions[40] is significant and similar in both cases. The $|v(\mathbf{r})|/g(\mathbf{r})$ ratio ($v(\mathbf{r})$ and $g(\mathbf{r})$ are, respectively, potential and kinetic energy density functions in the CP (3, −1)) reaches 1.27 and 1.38 for Fe−N and Fe−C interactions.

Interionic Interactions. The search for BCPs was also performed in the interionic area in crystalline **1**. It is found that all of the shortened contacts considered above correspond to attractive interactions. The bonding pattern formed by the cation−anion contacts and those linking sodium atoms and water molecules agrees well with the patterns expected from electrostatic consideration. Both cation−anion and Na−O interactions correspond to "peak-to-hole" type. The maxima of DED near

TABLE 1: Topological Parameters of $\rho(\mathbf{r})$ Distribution in BCPs of Interionic Interactions in 1

interaction	N^a	R, Å	$\rho(\mathbf{r})$, eÅ^{-3}	$\nabla^2\rho(\mathbf{r})$, eÅ^{-5}	$-v(\mathbf{r})$, a.u.	$h_e(\mathbf{r})$, a.u.	E_{cont}, kcal/mol
Na(1)···O(1W)	2	2.4721(6)	0.100	1.90	0.01170	0.00401	3.7
Na(2)···O(1W)	2	2.5084(6)	0.071	1.78	0.00909	0.00470	2.9
Na(1)···N(2)	2	2.4733(5)	0.102	1.99	0.01218	0.00424	3.8
Na(2)···N(3*)[b]	2	2.4702(6)	0.104	1.92	0.01210	0.00393	3.8
Na(1)···N(4″)[b]	2	2.5083(7)	0.092	1.74	0.01049	0.00381	3.3
Na(2)···N(4")[b]	2	2.4704(5)	0.106	1.98	0.01250	0.00402	3.9
O(1)···O(1A)	1	2.6423(5)	0.090	1.52	0.00960	0.00308	3.0
O(1)···N(3C)	4	3.2793(6)	0.034	0.43	0.00234	0.00104	0.7
N(2)···N(2B)	1	3.1751(6)	0.064	0.53	0.00427	0.00062	1.3
N(2)···N(4D)[b]	2	3.4544(5)	0.049	0.36	0.00282	0.00045	0.9
N(4)···O(1WE)	1	3.2548(6)	0.041	0.39	0.00248	0.00077	0.8

[a] The $N(3*)$, $N(4'')$, and $N(4D)$ atoms were obtained from the basic ones by means of symmetry operations $0.5 - x$, $0.5 + y$, $-0.5 - z$; $-x$, $-y + 1$, $-z + 1$; $x + 1$, y, z. [b] The $N(3*)$, $N(4'')$, and $N(4D)$ atoms were obtained from the basic ones by means of symmetry operations $0.5 - x$, $0.5 + y$, $-0.5 - z$; $-x$, $-y + 1$, $-z + 1$; $x + 1$, y, z.

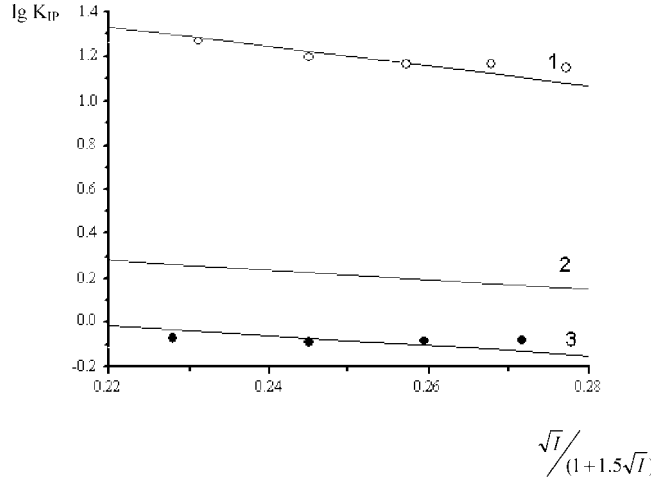

Figure 4. The stability constants of $Na^+,[Fe(CN)_6]^{4-}$ (○) and $Na+,[FeNO(CN)_5]^{2-}$ (●) ion pairs plotted against the ionic strength of solution. (1, 2) Values calculated by means of the Fuoss equation. (2,3) Accounting for the steric coefficient 0.5.

the oxygen and/or nitrogen atoms are extended in the direction of DED depletion around sodium cations. Such redistribution of electron density is, evidently, accompanied with the charge transfer from lone pairs (LPs) of either nitrogen atoms at the anion site or O(1W) atom to Na(1) and Na(2). On the other hand, although the major component of bond formation for cation−anion contacts is electrostatic attraction, the Na−O interactions exhibit the pronounced contribution of polarization effects. This results in a considerable polarization of water molecules. The evaluation of dipole moment for H_2O moiety in **1** leads to the value of 2.9 D, which is significantly higher than the corresponding value (1.85 D) for the isolated water molecule.[41] For comparison, the water dipole moment in the solid tetrahydrate of piperidine-2-carboxylic acid upon the formation of water layers reaches 3.4 D.[42]

In line with the topological parameters of $\rho(\mathbf{r})$ function in the corresponding BCPs the interionic interactions are all of closed-shell type (positive $\nabla^2\rho(\mathbf{r})$ values vary in the range of 1.74−1.99 eÅ^{-5}, and electron energy density $h_e(\mathbf{r})$ is 0.00381−0.00470 au (Table 1)). By use of the classification of bonded interactions proposed by Espinosa[40] the interionic bonds display a very small component of covalent character. In other words, it is practically negligible, and thus the cation−anion interactions in **1** can be considered as purely electrostatic ones. This approximation allows us to speculate about the character of binding between the ions of opposite charge in liquid phase through the application of Fuoss equation.[43] The latter is usually used to calculate the constant of ion pair formation and thus to describe the character of outer-sphere electrostatic interactions in the case of spherical charged particles. The interactions of the $[FeNO(CN)_5]^{2-}$ anion, as well as its isoelectronic analogue $[Fe(CN)_6]^{4-}$, with Na cations were investigated by means of potentiometry using the sodium electrode. The experimental values of stability constants for ion pairs of the $Na^+,[Fe(CN)_6]^{4-}$ type (Figure 4) coincide with ones estimated through the Fuoss equation, indicating the validity of the latter to describe the cation−anion interactions in the systems containing the nonspherical (octahedral) species. In the case of the Na^+, $[FeNO(CN)_5]^{2-}$ pairs the measured values were found to be two times smaller than those calculated for the electrostatic interactions within the two-charged-spheres model. Such difference in stability constants experimentally and theoretically obtained is, probably, resulted from the tendency of sodium cations to interact with cyano-groups rather than NO ones due to electrostatic reasons, i.e., the pronounced negative charge on the CN moieties. As a consequence, the cation−anion association in solutions is governed solely by Na···N−C bonding interactions being in a good agreement with the solid-state data. Thus, crystalline solids can serve as the model systems for investigating the behavior of molecules and/or ions in liquids and vice versa.

What is of paramount importance is the occurrence of the O···O and O···CN interactions between negatively charged species in the crystal of **1** proposed on the basis of the geometrical criteria. Taking into account the electron density distribution for the complex anion (Figure 3B) and the mutual disposition of the interacting NO groups, the O···O contact results from the overlap of oxygen LPs similar to the previously reported case of $MgCO_3$.[44] The DED peaks in the vicinity of O(1) and symmetry related O(1A) are directed toward each other (Figure 5A). The lines connecting LPs with nucleus for interacting atoms are tilted from the interatomic line by ca. 40°. Thus, the O···O bonds between the anionic species in **1** resembles the $Cl^-\cdots Cl^-$ contacts in the crystal of hydroxylammonium chloride[19] and can be attributed to the dispersion interactions.[45]

The character of O···CN bonding is completely different. It concerns, in addition to elongated interatomic separations, the number of interactions per one NO moiety equal to 4 and the character of electron density distribution. Although the bond path is located between oxygen and nitrogen atoms, whole C(2)N(3) fragment is, apparently, involved in the interaction with NO group acting as both donor and acceptor of electron density. The DED distribution in the area considered (Figure 5B) can be described as the interaction between LP of O(1) atom and π^* orbital of CN group of the neighboring anion. The opposite situation is realized in the case of the nitrogen belonging to this cyano group.

Thus, it can be assumed that the predominant component of these interactions is the charge transfer from LP of oxygen to carbon atom and from LP of nitrogen to O(1). The latter interaction is expected to be reflected in integral characteristics of the above atoms. For instance, such redistribution of $\rho(\mathbf{r})$ has to affect their atomic charges, i.e., to cause the accumulation of charge density in the case of carbon and its decrease on nitrogen as compared with other CN groups. To compute the

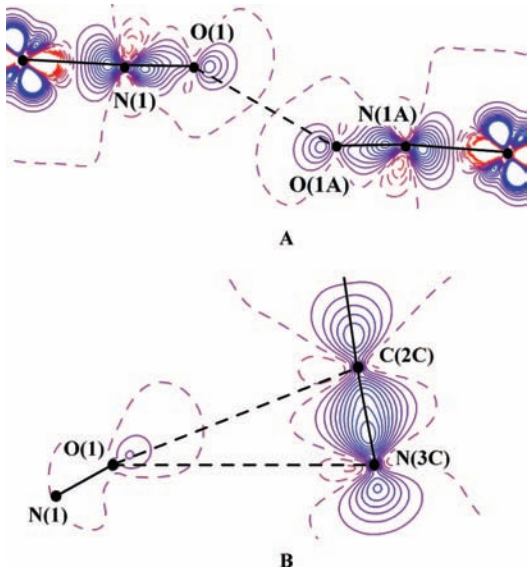

Figure 5. The DED sections in the planes of N−O···O−N and N−O···N−C interactions. Contours are drawn with 0.1 eÅ^{-3} steps; the nonpositive contours are dashed. The atoms labeled with A and C are obtained from the basic ones by the symmetry operations $-x-1$, $-y+2$, $-z+1$, and $x-1$, y, z.

corresponding atomic charges and to test the above hypothesis, we determined the atomic basins ($\mathbf{\Omega}$)[10] surrounded by a zero flux surface and integrated $\rho(\mathbf{r})$ over $\mathbf{\Omega}$.

Atomic Characteristics of Nitroprusside Moiety. The atomic charges (q) estimated according to this procedure equal +0.90, −0.32, and −0.02 e for Fe, O(1), and N(1) atoms, respectively, and vary from −1.17 to −0.98 and from 0.57 to 0.67 e for the rest of nitrogens and carbons, respectively. The minimum charge (−0.98 e) is found for the N(3) atom, whereas the most positively charged carbon is C(2). Thus, although the O···CN interactions clearly contribute to the charge redistribution in the crystal of **1**, the latter it is mainly due to cation−anion contacts. Indeed, the summation of atomic charges for cyano groups revealed that the C(2)N(3) moiety ($q = -0.30$) differs markedly from the two others ($q = -0.64$ and −0.54 for N(2) and N(4) atoms, respectively). This effect results from the quantitative and qualitative differences (see above) between interionic interactions formed by each CN fragment.

The net charge of the NO fragment is −0.34 e, which disagrees with the positive value commonly accepted for it.[46] On the other hand, the observed ν(N−O) in $[Fe(CN)_5NO]^{2-}$ is very close to that of the neutral NO[46] and can hardly be considered as the indicator of positively charged nitroso group in **1**. Thus, although the negative charge on the N(1)O(1) is not supported by any other physical chemical method, it does not contradict with the previously reported experimental data. The value of q for the NO moiety in **1** also agrees with the theoretical investigations of the nitroprusside anion.[47] However, since the previous theoretical studies were limited only to the examination of Mulliken or NBO charges, it was of interest to analyze those obtained by the integration of $\rho(\mathbf{r})$ over $\mathbf{\Omega}$ for the isolated anion **1**.

The quantum chemical calculations performed at different levels of theory (see Experimental section) revealed the strong level dependence of both the geometry and atomic characteristics for nitroprusside moiety. In particular, Fe−N and Fe−C distances varied in a very broad range with systematic shortening of Fe−N and elongation and equalization of Fe−C. Only the B3PW91/6-311G* (with account for solvent effects) data provided the reasonable geometrical parameters for anion. The corresponding Fe−N (1.644 Å) and N−O (1.129 Å) bond lengths were found to be relatively close to the experimental values. This is also true for the topological parameters in the BCPs of intraionic interactions, namely, the $\rho(\mathbf{r})$ and $\nabla^2\rho(\mathbf{r})$ are 1.267 eÅ^{-3} and 29.4 eÅ^{-5} for the Fe−N bond and in the range of 0.744−0.747 eÅ^{-3} and 5.73−6.71 eÅ^{-5} for Fe−C ones. In this case the nitroso group is positively charged with the corresponding values (Mulliken, NBO, and Bader) of +0.12, +0.23, and +0.01 e, and those on the oxygen atom are equal to −0.08, −0.079, and −0.33 e, respectively. The charge parameters calculated using different methods (Mulliken, NBO, and Bader) agree qualitatively. The charge on the nitroso group is equal to +0.12, +0.23, and +0.01 e, respectively, calculated using Mulliken, NBO, and Bader approach/scheme. All methods result in the positive q value for nitrogen atom of NO moiety and in a negative charge on oxygen. One notes that the charge parameters computed using different methods do not have to coincide, since the Bader's charges are not pointlike and, in general, appear to be larger at absolute scale, and the direct comparison of atomic charges calculated by three totally different approaches can be misleading. On the other hand, the Bader's theory is more theoretically sound[48] and, therefore, provides more reliable charge parameters. The latter should hold for the value of −0.34 e on nitroso group, although there is no reference data on NO Bader's charge for this particular anion. Therefore, further investigations of the electron density distribution in the system under study, including the analysis of atomic characteristics such as Bader's charges, are needed to put our results together with the vibration frequencies for the nitroso group.

In addition to level and basis set dependence, the theoretical atomic charge parameters suffer from the drastic changes of charge distribution upon the variation of the geometry of the anion. The atomic charges for the NO fragment calculated for the X-ray geometry of nitroprusside ion led to the values of different sign depending on the computational method (−0.05, +0.05, and −0.16 e for Mulliken, NBO, and Bader methods, respectively). One can see a clear tendency to more pronounced negative charge on the nitroso group when the theoretical Fe−N and N−O distances approach the experimental ones. Moreover, although the account for the nonspecific solvation results (B3PW91 calculations within the SCRF/PCM model) in the redistribution of the charge density to the NO fragment, there is still a significant discrepancy between the charges in crystal and in the model medium. This indicates the important role of specific solvation, which leads to practically the same negative charge on all of the anions forming the fist coordination sphere of iron atom in crystalline **1**. Nevertheless, the absolute value of charge on oxygen atom is ca. two times smaller than those for nitrogens of the cyano moieties, and thus, the cation−anion interactions preferably occur through the CN···Na binding.

On the other hand, water molecules in the crystal of **1** are charged positively (+0.05 e). The small value of the charge is due to the charge transfer resulted from the Na−OH_2 association and the absence of H-bonds. Therefore, the atomic charges can be used for the indirect investigation of the chemical bonding peculiarities, even concerning the anion−anion association. However, "easy-to-see" proof of the latter provided by another integrated property that is atomic volumes. Their values in the crystal of **1** obtained according to the procedure analogous to that for the estimation of charges[10] are rather accurate, and their sum in the crystal (281.83 Å^3) reproduces the unit cell volume

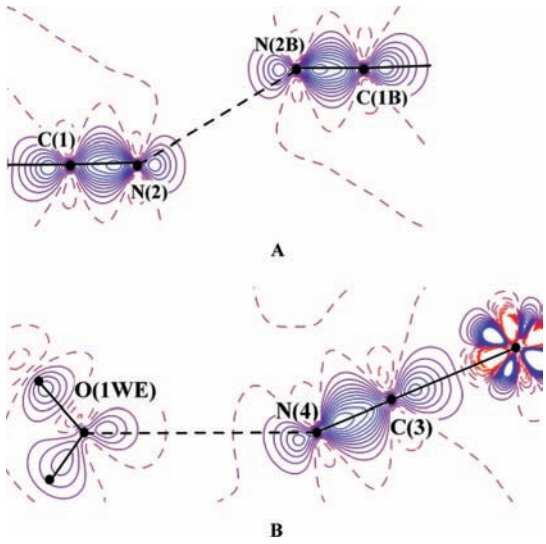

Figure 6. The DED distribution in the planes, containing C−N···N−C and anion−water interactions. Contours are drawn with 0.1 eÅ^{-3} step, the nonpositive contours are dashed. The atoms labeled with B and E are obtained from the basic ones by the symmetry operations $-x + 1$, $-y + 1$, $-z + 1$ and $-x$, $-y + 1$, $-z + 2$.

per formula moiety (282.82 Å^3) with the relative error smaller than 0.4%. Intuitively obvious result is that the anion is characterized by a larger volume (208.21 Å^3) than that of the cation (19.42 Å^3). This is rather common for ionic systems exhibiting the anion−anion interactions in solutions[4] as well as in the solid state.[13,49]

Anion−Anion Assembly: Quantitative Description. To describe the strength of the interactions between anionic species a simple parameter can be derived from the above atomic charges. As such a characteristic that can in theory provide the information about the strength of anion−anion interactions, the total charge of the complex anion can serve, which in our case is equal to −1.75 e, that is considerably larger than the corresponding value for urea nitrate.[21] This along with the smaller interanionic distances makes it difficult to predicting the energy of anion-anion bonding. On the other hand, the small value of charge transfer (0.25 e) indicates the relative weakness of the cation−anion interactions.

In addition to the above types of anionic assembly, a number of BCPs corresponding to considerably long anion−anion and anion−water interactions were found (Table 1). In particular, symmetry equivalent CN(2) species with the minimal separation of 3.1751(6) Å are bonded in such a manner that these interactions are geometrically similar to those between nitroso-groups. Moreover, they show practically the same DED distribution as the O···O bonding, that is "peak to peak" type with the tilt angle equal to ∼40° (Figure 6A). The C(3)N(4) group is also not an exception. It participates in the formation of two attractive interactions with the above CN(2) fragment, which are characterized by substantially elongated N···N distance (3.4544(5) Å) as compared to that between the symmetry equivalent CN(2) species. The DED distribution of this interaction is also attributed to the "peak to hole" type.

Besides the anion−anion bonding, an unusual CN···OH$_2$ assembly (N···O 3.2548(6) Å) with C(3)N(4) group was observed. According to the DED in the relevant region (Figure 6B), such interaction can be attributed to the "peak to peak" type, thus indicating its formation through the overlap of LPs of oxygen and nitrogen.

Summarizing the forgoing results, the interactions between species with the same and different sign of charge, although contrasting sharply both in DED distributions and in their character are similar in number and in weakness according to the value of the charge transfer and in formally repulsive nature of bonding between anions. As a result, one can expect them to be comparable on the quantitative level.

It is important to indicate that although the detection of interionic interactions and determination of the types of corresponding associates can easily be accomplished by means of EAS analysis, conventional X-ray, or even ionometric data, but they cannot provide the quantitative characterization of chemical binding in the system studied. However, it is the most important advantage of close examination of experimental electron density functions.

Accordingly, the energy of the interionic interactions (E_{cont}) in the crystal of **1** was estimated on the basis of the Espinosa's correlation[11,12] that relates the E_{cont} with the value of potential energy density $v(\mathbf{r})$ in the corresponding BCPs. Thus, the cation−anion and cation−water contacts were found to be relatively weak and characterized by the E_{cont} of 2.9−3.9 kcal/mol (Table 1). This is consistent with the small value of charge transfer (see above). The strength of the O···O interactions between the negatively charged species is practically the same (3.0 kcal/mol) and exceeds by far the corresponding interaction (1.3 kcal/mol) in the crystalline urea nitrate.[21] This effect, apparently, results from the equivalency of the charge density accumulation on oxygen atom in **1** ($q = -0.32$ e) and urea nitrate (q is from −0.37 to −0.33) along with the difference in interatomic distance, where considerable shortening leads to more effective overlap of LPs of oxygens in the case of nitroprusside anions. Such considerations holds for danburite crystal,[20] where the absolute value of charge on oxygens is larger (−1.90 to −1.86 e) and the O···O distances are even shorter than 2.6 Å.

The E_{cont} values for other anion−anion bonds in **1** are smaller (0.7−1.3 kcal/mol) but of the same order of magnitude as the corresponding values for the Na−N and Na−O bonds. This clearly shows that this type of bonding contributes considerably to the lattice energy of the crystalline solid considered. In other words, cation−anion or cation−water and anion−anion contacts are equally responsible for the stability of crystal of **1**. Indeed, the summation of E_{cont} for the interionic bonds per one formula unit provide us with the values of 29.7 and 13.1 kcal/mol for Na−N and Na−O bonds and 9.1 and 0.8 kcal/mol for the anion−anion and anion−water associations, respectively. The energy of the interactions between nitroprusside anions in **1** gives rise to 31% of the total E_{cont} for cation−anion bonds or is equal to 17% of the energy of all of the contacts.

Therefore, one can conclude that the chemical bonding between nitroprusside anions is the common feature of corresponding solids and can even occur in liquid systems. The bonding energy is of the same order of magnitude as that of the conventional cation−anion bonds in their alkaline salts. This indicates that such interactions should not be neglected in "constructing" specific architectures on the basis of the nitroprusside moiety. Moreover, significant fraction of the anion−anion binding in this particular crystal demonstrates that such type of interactions, competes with the conventional electrostatically favorable ones in crystal packing formation, and, hence, is important for directional design of ionic materials.

Conclusion

Topological analysis of the electron density distribution in **1** revealed that the interactions between anions not only realize in the crystals but also contribute greatly to the stability of the

solids and, thus, affect their physicochemical properties such as electronic properties, which can be detected in EAS spectra of the corresponding salts. Unfortunately, so far the proof of the occurrence of anion−anion interactions provided by AIM investigation may be a little confusing for the majority of chemists. Its results, being in general more informative than those of any other physical method, are considered with skepticism. The EAS analysis is less abstract and easier to understand. On the other hand, both methods confirm the possibility of bonding between species with the same sign of charge in condensed state. If the results of EAS investigation are accepted even for the systems consisting of two different anions (complex and reducing ones), one has to take for granted the AIM data, indicating the formation of such interactions in a number of ionic crystals. Moreover, taking into account the perfect agreement between AIM results and "chemical common sense" in the case of conventional bonds,[45] there is no logical reason to deny the importance of anion−anion or cation−cation contacts for crystal stabilization, especially when they are comparable with the former in energy.

Accordingly, the AIM analysis of $\rho(\mathbf{r})$ distribution is a more powerful approach to simultaneously describing the bonding between likely-charged ions on qualitative and quantitative levels. However, EAS data is a very convenient source of information concerning the presence of anion−anion interactions, if the crystalline material is not available or its quality is not good enough to perform the high-resolution X-ray experiment and subsequent topological analysis of electron density.

Acknowledgment. This study was financially supported by the Russian Foundation for Basic Research (Project 06-03-32557), the Foundation of the President of the Russian Federation (Federal Program for the Support of Leading Scientific Schools, Grant NSh 1060.2003.30, and Young Doctors, Grant MK-1054.2005.3), and the Russian Science Support Foundation. Authors thank Dr. Evgeny Pidko (Eindhoven University of Technology) for fruitful discussion.

Supporting Information Available: Monopole and multipole populations, local symmetry, atomic coordinates, anisotropic displacement parameters, and differences of mean-squares displacement amplitudes. This material is available free of charge via the Internet at http://pubs.acs.org.

References and Notes

(1) Braga, D.; Grepioni, F.; Novoa, J. J. *Chem. Commun.* **1998**, 1959.
(2) Carvajal, M.; Garcia-Yoldi, I.; Novoa, J. J. *THEOCHEM* **2005**, *727*, 181.
(3) Krot, N. N.; Grigoriev, M. S. *Russ. Chem. Rev.* **2004**, *73*, 89.
(4) Kotov, V. Y.; Gorel'sky, S. I. *Russ. Chem. Bull.* **1999**, *48*, 823.
(5) Gorel'skii, S. I.; Kim, T. G.; Klimova, T. P.; Kotov, V. Y.; Lokshin, B. V.; Perfil'ev, Y. D.; Sherbak, T. I.; Tsirlina, G. A. *Mendeleev Commun.* **2000**, 6.
(6) Alkorta, I.; Elguero, J. E. *Structural Chemistry* **2004**, *15*, 117.
(7) Koritsanszky, T. S.; Coppens, P. *Chem. Rev.* **2001**, *101*, 1583.
(8) Gatti, C. *Z. Kristallograph.* **2005**, *220*, 399.
(9) Tsirelson, V. G.; Ozerov, R. P. *Electron density and Bonding in Crystals: Principles, Theory and X-Ray Diffraction experiments in Solid State Physics And Chemistry*; IOP Publishing Ltd.: Bristol and Philadelphia, 1996.
(10) Bader, R. F. W. *Atoms In molecules. A Quantum Theory*; Clarendron Press: Oxford, 1990.
(11) Espinosa, E.; Molins, E.; Lecomte, C. *Chem. Phys. Lett.* **1998**, *285*, 170.
(12) Espinosa, E.; Alkorta, I.; Rozas, I.; Elguero, J.; Molins, E. *Chem. Phys. Lett.* **2001**, *336*, 457.
(13) Pendas, A. M.; Costales, A.; Luana, V. *J. Phys. Chem. B* **1998**, *102*, 6937.
(14) Gibbs, G. V.; Boisen, M. B.; Rosso, K. M.; Teter, D. M.; Bukowinski, M. S. T. *J. Phys. Chem. B* **2000**, *104*, 10534.
(15) Tsirelson, V. G.; Zou, P. F.; Tang, T. H.; Bader, R. F. W. *Acta Cryst. A* **1995**, *51*, 143.
(16) Zhurova, E. A.; Tsirelson, V. G.; Stash, A. I.; Pinkerton, A. A. *J. Am. Chem. Soc.* **2002**, *124*, 4574.
(17) Matta, C. F.; Castillo, N.; Boyd, R. J. *J. Phys. Chem. B* **2006**, *110*, 563.
(18) Gibbs, G. V.; Downs, R. T.; Cox, D. F.; Ross, N. L.; Boisen, N. B.; Rosso, K. M. *J. Phys. Chem. A* **2008**, *112*, 3693.
(19) Nelyubina, Y. V.; Antipin, M. Y.; Lyssenko, K. A. *J. Phys. Chem. A* **2007**, *111*, 1091.
(20) Luana, V.; Costales, A.; Mori-Sanchez, P.; Pendas, A. M. *J. Phys. Chem. B* **2003**, *107*, 4912.
(21) Nelyubina, Y. V.; Lyssenko, K. A.; Golovanov, D. G.; Antipin, M. Y. *Cryst. Eng. Comm.* **2007**, *9*, 991.
(22) Nelyubina, Y. V.; Lyssenko, K. A.; Kostyanovsky, R. G.; Bakulin, D. A.; Antipin, M. Y. *Mendeleev Commun.* **2008**, *18*, 29.
(23) Navaza, A.; Chevrier, G.; Alzari, P. M.; Aymonino, P. J. *Acta Cryst. C* **1989**, *45*, 839.
(24) Antipin, M. Y.; Tsirelson, V. G.; Flugge, M.; Struchkov, Y. T.; Ozerov, R. P. *Chem. Script.* **1986**, *26*, 477.
(25) Nikolskii, A. B.; Kotov, V. Y. *Mendeleev Commun.* **1995**, 139.
(26) Nikolskii, A. B.; Kotov, V. Y. *Russ. J. Coord. Chem.* **1997**, *23*, 706.
(27) The data can be obtained free of charge via www.ccdc.cam.ac.uk/conts/retrieving.html (or from the Cambridge Crystallographic Data Centre, 12, Union Road, Cambridge CB2 1EZ, UK; fax +44 1223 336033; deposit@ccdc.cam.ac.uk).
(28) Hansen, N. K.; Coppens, P. *Acta Crystallogr., Sect. A* **1978**, *34*, 909.
(29) Koritsansky, T. S.; Howar, S. T.; Richter, T.; Mallinson, P. R.; Su, Z.; Hansen, N. K. X. D. *A computer program package for multipole refinement and analysis of charge densities from X-ray diffraction data*. 1995.
(30) Su, Z. W.; Coppens, P. *Acta Crystallogr., Sect. A* **1995**, *51*, 27.
(31) Kirzhnits, D. A. *Sov. Phys. JETP* **1957**, *5*, 54.
(32) Stash, A.; Tsirelson, V. *J. Appl. Crystallogr.* **2002**, *35*, 371.
(33) Miertus, S.; Tomasi, J. *Chem. Phys.* **1982**, *65*, 239.
(34) Popelier, P. L. A.; Bone, R. G. A. *MORPHY98*: UMIST, England, EU.
(35) Ferlay, S.; Holakovsky, R.; Hosseini, M. W.; Planeix, J. M.; Kyritsakas, N. *Chem. Commun.* **2003**, 1224.
(36) Gorelsky, S. I.; da Silva, S. C.; Lever, A. B. P.; Franco, D. W. *Inorg. Chim. Acta* **2000**, *300*, 698.
(37) Kurki-Suonio, K. *Isr. J. Chem.* **1977**, *16*, 124.
(38) Aldoshin, S. M.; Lyssenko, K. A.; Antipin, M. Y.; Sanina, N. A.; Gritsenko, V. V. *J. Mol. Struct.* **2008**, *875*, 309.
(39) Caramori, G. F.; Frenking, G. *Organometallics* **2007**, *24*, 5815.
(40) Espinosa, E.; Alkorta, I.; Elguero, J.; Molins, E. *J. Chem. Phys.* **2002**, *117*, 5529.
(41) Glendening, E. D. *J. Phys. Chem. A* **2005**, *109*, 11936.
(42) Lyssenko, K. A.; Nelyubina, Y. V.; Kostyanovsky, R. G.; Antipin, M. Y. *Chem. Phys. Chem.* **2006**, *7*, 2453.
(43) Fuoss, R. M. *J. Am. Chem. Soc.* **1958**, *80*, 5059.
(44) Gottlicher, S.; Vegas, A. *Acta Cryst., Sect. B* **1988**, *44*, 362.
(45) Bader, R. F. W. *J. Phys. Chem. A* **1998**, *102*, 7314.
(46) Manoharan, P. T.; Gray, H. B. *J. Am. Chem. Soc.* **1965**, *87*, 3340.
(47) Soria, D. B.; Piro, O. E.; Varetti, E. L.; Aymonino, P. J. *J. Chem. Cryst.* **2001**, *31*, 471.
(48) Bader, R. F. W.; Matta, C. F. *J. Phys. Chem. A* **2004**, *108*, 8385.
(49) Luana, V.; Costales, A.; Pendas, A. M. *Phys. Rev. B* **1997**, *55*, 4285.

JP803394F